Supporting Information for:

Structure and Properties of an Eight-Coordinate Mn(II) Complex that Demonstrates a High Water Relaxivity

Koustubh S. Dube and Todd C. Harrop*

Department of Chemistry, The University of Georgia, Athens, Georgia, USA 30602

*E-mail: tharrop@uga.edu

Experimental

General Information. All reagents were purchased from commercial suppliers and used as received unless otherwise noted. Acetonitrile (MeCN), methylene chloride (CH_2Cl_2), and diethyl ether (Et_2O) were purified by passing over activated alumina columns in an MBraun MB-SPS solvent purification system. Ethanol (EtOH) was purified by anaerobically distilling over $Mg(OEt)_2$. Millipore water was obtained from a Barnstead Nanopure Infinity Ultrapure water system (resistivity at 298 K: 18.3 MΩ•cm; 0.2 μm filter assembly). The ligand, (N^1E,N^2E)-N^1,N^2-bis((1-methyl-1H-imidazol-2-yl)methylene)benzene-1,2-diamine (L_{N4}), was prepared and checked according to the published procedure.[1] Unless specified, all reactions and spectroscopic studies were performed under an inert atmosphere of N_2(g) using standard Schlenk-line techniques or in an MBraun Labmaster glovebox under an atmosphere of purified N_2.

Physical Methods. FTIR spectra were collected with a ThermoNicolet 6700 spectrophotometer running the OMNIC software program. All samples were run as solids either as a KBr pellet or on an ATR (attenuated total reflectance) diamond transmission window. X-band EPR was recorded on a Bruker ESP 300E EPR spectrophotometer controlled by a Bruker microwave bridge. The EPR was equipped with a continuous-flow liquid He cryostat and a temperature controller made by Oxford Instruments. Electronic absorption spectra were recorded at 298 K in the specified solvent on a Cary-50 UV-vis spectrometer with a Quantum Northwest TC 125 temperature controller. Solution pH readings were recorded with an Accumet Model 25 pH/ion meter with a mercury-free glass electrode, which was calibrated using the standard three buffer system (pH = 4, 7, and 10). Cyclic voltammetry (CV) measurements were performed with 2.7 mM analyte on a PAR Model 273A potentiostat using a Ag/Ag^+ reference electrode (0.01 M $AgNO_3$ in 0.1 M $^nBuN_4PF_6$ in MeCN; $E_{1/2}$ (ferrocene/ferrocenium) = 0.09 V at RT), Pt-wire

counter electrode, and a Glassy Carbon working electrode (2 mm diameter). NMR spectra were recorded at 298 K on either a 400 MHz Bruker BZH 400/52 NMR spectrometer or on a Varian Unity Inova 500 MHz NMR spectrometer. Magnetic susceptibility measurements were performed in the solid-state using a Johnson-Matthey magnetic susceptibility balance and in the solution-state (CD_3CN) at 298 K using the Evans method on a Varian Unity Inova 500 MHz NMR spectrometer.[2] ESI-MS data were collected on a Perkin-Elmer Sciex API I Plus quadrupole mass spectrometer. Elemental analysis for C, H, and N was performed by QTI-Intertek using a Perkin-Elmer 2400 CHN analyzer.

[Synthesis of the Compounds]

Synthesis Safety Note: *Although no problems were observed in this work, perchlorate (ClO_4^-) salts of transition metals are potentially explosive and should be handled with care.*

$[Mn(L_{N4})_2](ClO_4)_2$ (1). To a dark orange solution of L_{N4} (0.3685 g, 1.261 mmol) in 5 mL of MeCN was added a 5 mL MeCN solution of $[Mn(H_2O)_6](ClO_4)_2$ (0.1601 g, 0.4424 mmol) at room temperature (RT). The resulting yellow colored solution was stirred for 4 h at RT after which the MeCN was reduced to 2 mL by rotary evaporation. Addition of ~5 mL of Et_2O to the above solution resulted in a yellow precipitate. This solid was filtered on a medium porosity sintered glass frit and washed with ~2 mL of Et_2O. Yellow crystals of complex **1** were formed by slow diffusion of Et_2O into a solution of **1** in MeCN at -5 °C, 0.3033 g (0.3617 mmol, 82%). FTIR (ATR-diamond, solid-state) ν_{max} (cm^{-1}): 3118 (w), 1615 (m), 1581 (w), 1530 (w), 1484 (s), 1440 (s), 1414 (m), 1371 (w), 1325 (m), 1286 (m), 1227 (w), 1160 (w), 1074 (vs, ClO_4), 952 (s), 939 (s), 886 (s), 757 (s), 708 (w), 667 (m), 620 (s), 596 (m), 560 (w), 543 (w). UV-vis (MeCN, 298 K), λ_{max}, nm (ε, M^{-1} cm^{-1}): 315 (45,000), 368 (21,000). μ_{eff}: 4.81 BM (solid-state), 5.76 BM (solution-state in CD_3CN). LRMS-ESI (*m/z*): $[M - 2\ ClO_4]^{2+}$ calcd for $C_{32}H_{32}N_{12}Mn$, 319.6;

found, 319.6. E_{red} (irreversible $Mn^{II/I}$, MeCN, RT, versus Fc/Fc^{+}): –1.68 V. Anal. Calcd for $C_{32}H_{32}N_{12}Cl_2O_8Mn{\bullet}CH_3CN$: C, 46.43; H, 4.01; N, 20.70. Found: C, 46.27; H, 3.68; N, 20.62.

Stability of $[Mn(L_{N4})_2](ClO_4)_2$ (1) in aqueous media. To test the stability of complex **1** in aqueous solution, we monitored the change in its UV-vis spectrum upon dissolution in different buffered solutions at 298 K under aerobic conditions. The complex was made as a stock solution in MeCN and an aliquot of this (50 μL) stock was added to a UV-vis cell containing 3 mL of the appropriate buffer. After addition, the UV-vis spectrum was recorded for 2 h at 1 min intervals (see Figs. S1-S4). For all buffers tested, the intensity of λ_{max} ~315 nm gradually decreased with the appearance of an isosbestic point at ~300 nm and a new blue-shifted peak at ~290 nm. The lower intensity peak at 370 nm also decreased. After this initial decrease, the λ_{max} 290 nm increased slightly and appears to maximize with complete decrease of the λ_{max} 370 nm band. For CHES and phosphate buffer, the data were fit using the monophasic pseudo-first order rate equation: $y = A_0 + (A_\infty – A_0) * (1–\exp(-kt))$, where A_∞ and A_0 are absorbance at time $t = \infty$ (i.e. when reaction is complete) and at t = 0 s, respectively, and y = absorbance at the specified wavelength. For MES and PIPES buffer, the data were fit using a two phase model: $y = A_0 + (A_\infty – A_0) * a(1–\exp(-k_{obs\text{-}fast}t)) + b(1–\exp(-k_{obs\text{-}slow}t))$ where $a = (A_\infty – A_0) *$ (%fast) * 0.1 and $b = (A_\infty – A_0) *$ (%slow) * 0.1. The average rate constants (k_{obs}) with their standard deviations were calculated from triplicate runs under identical experimental conditions.

The result of the aqueous reaction was verified by liquid-liquid extraction of the aqueous mixture with CH_2Cl_2 and characterization of the organic soluble fraction (sample procedure): After 2 h reaction in aqueous buffer (same time as the UV-vis studies), the yellow aqueous solution was transferred to a separatory funnel where it was extracted with 3 × 5 mL of CH_2Cl_2. The yellow organic layer was then dried over anhydrous $MgSO_4$, filtered, and roto-vapped to

afford a yellow residue. This material was subjected to LR-ESI-MS and UV-vis analysis, which revealed the presence of complex **1** (Fig. S9).

Stability of 1 in phosphate buffer (pH = 7.27). A 5 mM stock solution of phosphate buffer (pH 7.27) was freshly prepared in millipore water and a 0.775 mM stock of complex **1** was prepared in MeCN. A 50 μL aliquot of the complex **1** stock was then added to 3 mL of the phosphate buffer solution in a quartz UV-vis cuvette and the UV-vis was monitored for 2 h at 1 min intervals (see Fig. S1); $k_{obs} = 6.53 \pm 0.28 \times 10^{-4}$ s^{-1} at 294 nm.

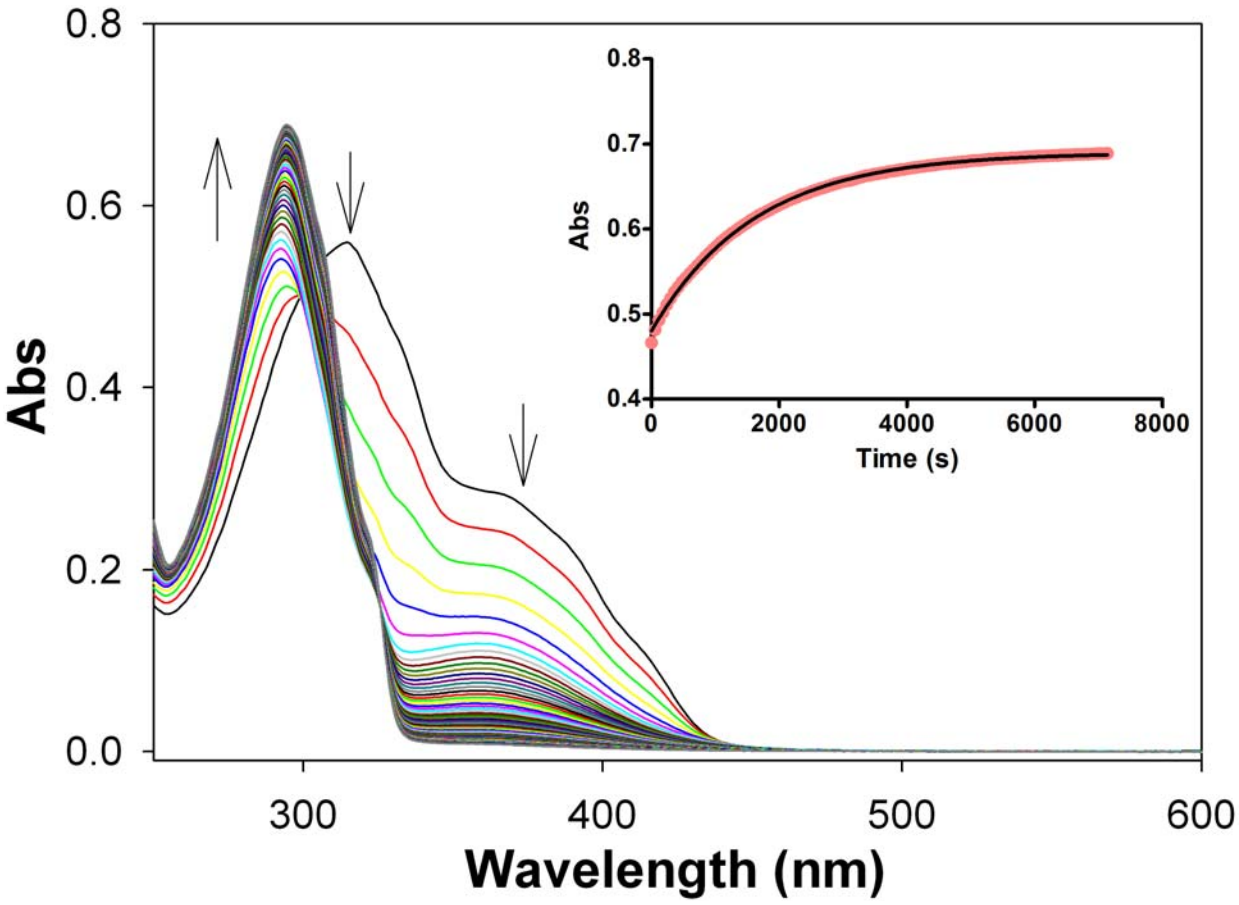

Fig. S1. UV-vis spectral monitoring of complex **1** (0.013 mM) in phosphate buffer (pH = 7.27) at 298 K with arrows showing direction of change (data collected at 1 min intervals but only every 2 min plot is displayed for clarity in the UV-vis, total time =120 min); inset shows A_{294} vs. time plot that the kinetic parameters were derived from (data in red, fit = black line).

Stability of 1 in PIPES buffer (pH = 7.31). A 50 mM stock solution of PIPES buffer (pH = 7.31) was freshly prepared in millipore water and a stock of 0.800 mM complex **1** was prepared in MeCN. A 50 μL aliquot of the complex **1** stock was then added to 3 mL of PIPES buffer in a quartz UV-vis cuvette and the UV-vis was monitored for 2 h at 1 min intervals (see Fig. S2); k_{obs} (fast) = 2.06 ± 0.02 × 10^{-3} s^{-1}, k_{obs} (slow) = 6.89 ± 1.03 × 10^{-5} s^{-1} at 294 nm.

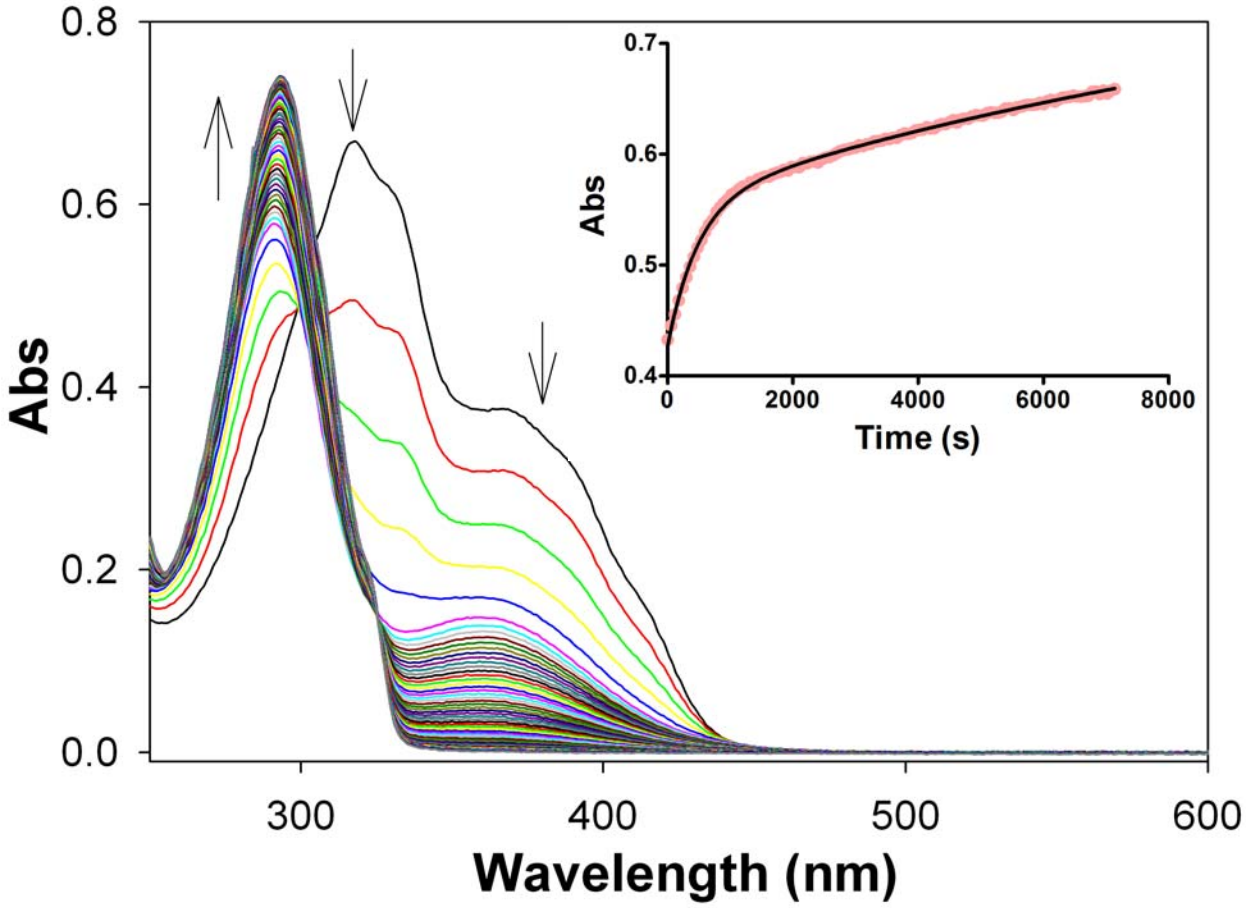

Fig. S2. UV-vis spectral monitoring of complex **1** (0.013 mM) in PIPES buffer (pH = 7.31) at 298 K with arrows showing direction of change (data collected at 1 min intervals but only every 2 min plot is displayed for clarity in the UV-vis, total time = 120 min); inset shows A_{294} vs. time plot that the kinetic parameters were derived from (data in red, fit = black line).

Stability of 1 in CHES buffer (pH = 9.04). A 50 mM stock solution of CHES buffer (pH = 9.04) was freshly prepared in millipore water and a stock of 0.800 mM complex **1** was prepared in MeCN. A 50 μL aliquot of the complex **1** stock was then added to 3 mL of CHES buffer in a quartz UV-vis cuvette and the UV-vis was monitored for 2 h at 1 min intervals (see Fig. S3); k_{obs} = 2.58 ± 0.55 × 10^{-3} s^{-1} at 291 nm.

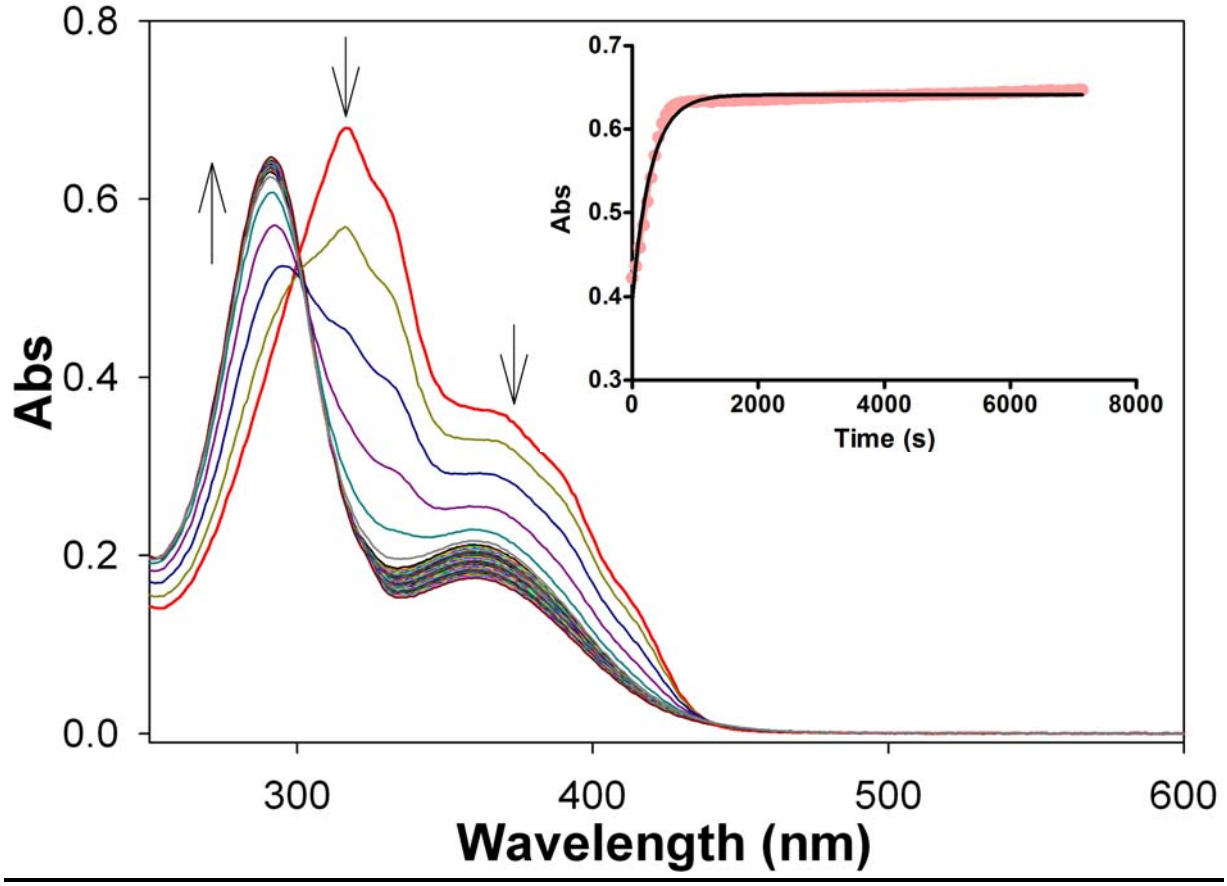

Fig S3. UV-vis spectral monitoring of complex **1** (0.013 mM) in CHES buffer (pH = 9.04) at 298 K with arrows showing direction of change (data collected at 1 min intervals but only every 2 min plot is displayed for clarity in the UV-vis, total time = 120 min); inset shows A_{291} vs. time plot that the kinetic parameters were derived from (data in red, fit = black line).

Stability of 1 in MES buffer (pH = 6.24). A 50 mM stock solution of MES buffer (pH = 6.24) was freshly prepared in millipore water and a stock of 0.800 mM complex **1** was prepared in MeCN. A 50 μL aliquot of the complex **1** stock was then added to 3 mL of MES buffer in a quartz UV-vis cuvette and the UV-vis was monitored for 2 h at 1 min intervals (see Fig. S4); k_{obs} (fast): $9.06 \pm 1.28 \times 10^{-3}$ s^{-1}, k_{obs} (slow): $2.91 \pm 0.07 \times 10^{-4}$ s^{-1} at 291 nm.

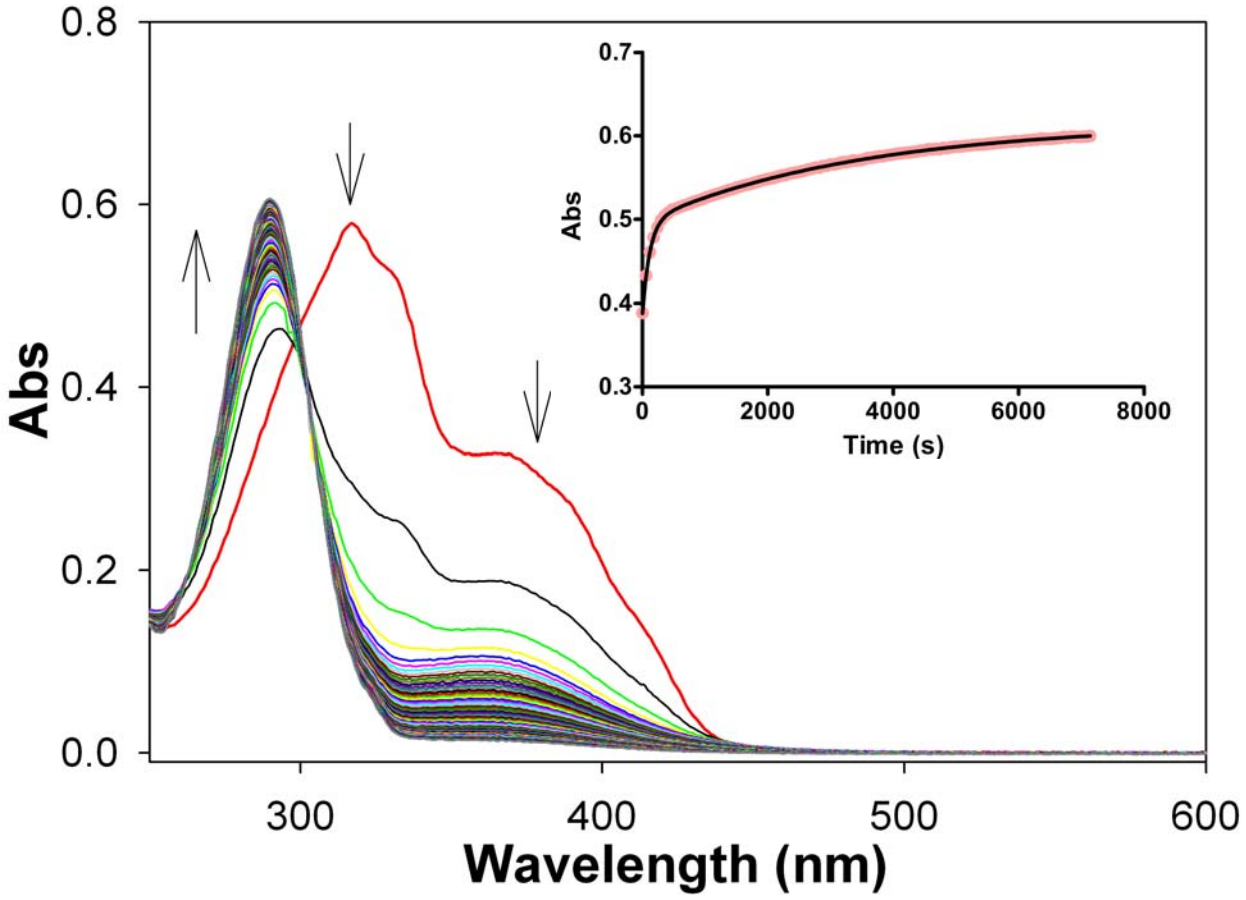

Fig. S4. UV-vis spectral monitoring of complex **1** (0.013 mM) in MES buffer (pH = 6.24) at 298 K with arrows showing direction of change (data collected at 1 min intervals but only every 2 min plot is displayed for clarity in the UV-vis, total time = 120 min); inset shows A_{291} vs. time plot that the kinetic parameters were derived from (data in red, fit = black line).

[Reactivity of Complex 1]

Reactivity of 1 with nitric oxide (NO). To an anaerobic MeCN solution (5 mL) of **1** (0.8478 g, 1.011 mmol) was purged NO(g) for 1 min and the solution was allowed to stir under an NO atmosphere. No visible color change was observed in the reaction flask over the next 30-45 min. The MeCN solvent was then removed by vacuum distillation and the yellow residue was stirred in Et_2O for 1 h. The yellow solid thus obtained was filtered, dried, and characterized. Spectroscopic measurements (LR-ESI-MS and FTIR) were identical to complex **1** indicating no reaction with NO(g).

Reactivity of 1 with sodium nitrite ($NaNO_2$). To a 1 mL MeCN solution containing **1** (0.0053, 0.0063 mmol) was added 0.0154 g (0.2232 mmol = 35 mol-equiv) of $NaNO_2$. The reaction slurry was stirred for 30 min at RT with no observable visible changes. After stirring the reaction mixture was filtered to remove unreacted $NaNO_2$ and the filtrate was subject to ESI-MS and UV-vis studies which revealed only complex **1**.

Reactivity of 1 with sodium chloride (NaCl). A similar procedure was used except reagents were 0.0059 g (0.0070 mmol) of **1** and 0.0154 g (0.2635 mmol = 38 mol-equiv) of NaCl. The reaction slurry was stirred for 30 min at RT with no observable visible changes. Reaction workup revealed only complex **1**.

Reactivity of 1 with tetraethylammonium chloride (Et_4NCl). To a 2 mL MeCN solution of **1** (0.011 mM) was added a 15 μL aliquot of a 14.5 mM MeCN solution of Et_4NCl (final concentration = 0.107 mM). The reaction was monitored at 1 h intervals for 10 h by UV-vis. Small changes do occur in the UV-vis, however, the ESI-MS of this reaction mixture revealed only **1** with no other products consistent with probable counter-anion exchange from $[Mn(L_{N4})_2](ClO_4)_2$ to $[Mn(L_{N4})_2]Cl_2$.

Reactivity of 1 with tetramethylammonium bromide (Me_4NBr). A similar procedure was used except solutions were 0.011 mM of **1** in MeCN and a 15 μL aliquot of a 13.0 mM MeCN solution of Me_4NBr (final concentration = 0.095 mM). Similar small changes in the UV-vis were obtained with ESI-MS showing only **1** consistent with probable counter-anion exchange from $[Mn(L_{N4})_2](ClO_4)_2$ to $[Mn(L_{N4})_2]Br_2$.

X-ray crystallographic data collection, structure solution, and refinement. Pale-yellow colored crystals of $[Mn(L_{N4})_2](ClO_4)_2$•MeCN (**1**•MeCN) were grown under aerobic conditions by slow diffusion of Et_2O into solutions of **1** in MeCN at -5°C. A suitable crystal was mounted and sealed inside a glass capillary. All geometric and intensity data were measured at 293 K on a Bruker SMART APEX II CCD X-ray diffractometer system equipped with graphite monochromatic Mo Kα radiation (λ = 0.71073 Å) with increasing ω (width 0.5° per frame) at a scan speed of 10 s/frame controlled by the SMART-APEX II software package.[3] The intensity data were corrected for Lorentz-polarization effects and for absorption[4] and integrated with the SAINT software package. Empirical absorption corrections were applied to structures using the SADABS program.[5] The structures were solved by direct methods with refinement by full-matrix least-squares based on F^2 using the SHELXTL-97 software[6] incorporated in the SHELXTL 6.1 software package.[7] The hydrogen atoms were fixed in their calculated positions and refined using a riding model. All non-hydrogen atoms were refined anisotropically. Selected crystal data for complex **1** is summarized in Table S1. Selected bond distances and angles for **1** are given in Table S2. Perspective views of the complexes were obtained using ORTEP.[8]

Table S1. Summary of crystal data and intensity collection and structure refinement parameters for $[Mn(L_{N4})_2](ClO_4)_2$•MeCN (**1**•MeCN).

Parameters	**1**•MeCN
Formula	$C_{34}H_{35}N_{13}O_8Cl_2Mn$
Formula weight	879.59
Crystal system	Monoclinic
Space group	$P2_1/c$
Crystal color, habit	Yellow, rectangle
a, Å	10.3455(6)
b, Å	21.1221(12)
c, Å	18.0690(10)
α, deg	90.00
β, deg	92.6490(10)
γ, deg	90.00
V, Å^3	3944.2(4)
Z	4
ρ_{calcd}, g/cm^{-3}	1.481
T, K	293(2)
abs coeff, μ, mm^{-1}	0.538
θ limits, deg	2.19-28.26
total no. of data	53897
no. of unique data	9736
no. of parameters	523
GOF on F^2	1.003
R_1,[a] %	6.47
wR_2,[b] %	16.70
max, min peaks, e/Å^3	0.721,-0.501

[a] $R_1 = \Sigma||F_o| - |F_c|| / \Sigma |F_o|$; [b] $wR_2 = \{\Sigma[w(F_o^2 - F_c^2)^2]/\Sigma[w(F_o^2)^2]\}^{1/2}$

Table S2. Selected bond distances (Å) and bond angles (deg) for $[Mn(L_{N4})_2](ClO_4)_2$•MeCN (**1**•MeCN).

Mn(1)-N(1)	2.319(3)	N(3)-Mn(1)-N(9)	135.33(11)
Mn(1)-N(3)	2.521(3)	N(3)-Mn(1)-N(10)	134.00(11)
Mn(1)-N(4)	2.443(3)	N(3)-Mn(1)-N(11)	79.89(11)
Mn(1)-N(5)	2.300(3)	N(4)-Mn(1)-N(5)	69.99(11)
Mn(1)-N(7)	2.333(3)	N(4)-Mn(1)-N(7)	82.91(12)
Mn(1)-N(9)	2.482(3)	N(4)-Mn(1)-N(9)	137.42(11)
Mn(1)-N(10)	2.496(3)	N(4)-Mn(1)-N(10)	137.88(11)
Mn(1)-N(11)	2.310(3)	N(4)-Mn(1)-N(11)	81.21(11)
N(1)-Mn(1)-N(3)	67.82(11)	N(5)-Mn(1)-N(7)	100.70(12)
N(1)-Mn(1)-N(4)	131.50(11)	N(5)-Mn(1)-N(9)	84.38(12)
N(1)-Mn(1)-N(5)	158.14(12)	N(5)-Mn(1)-N(10)	79.64(12)
N(1)-Mn(1)-N(7)	87.72(12)	N(5)-Mn(1)-N(11)	87.94(12)
N(1)-Mn(1)-N(9)	79.92(11)	N(7)-Mn(1)-N(9)	68.76(11)
N(1)-Mn(1)-N(10)	79.80(11)	N(7)-Mn(1)-N(10)	132.21(11)
N(1)-Mn(1)-N(11)	91.56(12)	N(7)-Mn(1)-N(11)	158.08(12)
N(3)-Mn(1)-N(4)	63.69(10)	N(9)-Mn(1)-N(10)	63.69(10)
N(3)-Mn(1)-N(5)	133.32(11)	N(9)-Mn(1)-N(11)	132.62(11)
N(3)-Mn(1)-N(7)	79.57(11)	N(10)-Mn(1)-N(11)	68.93(11)

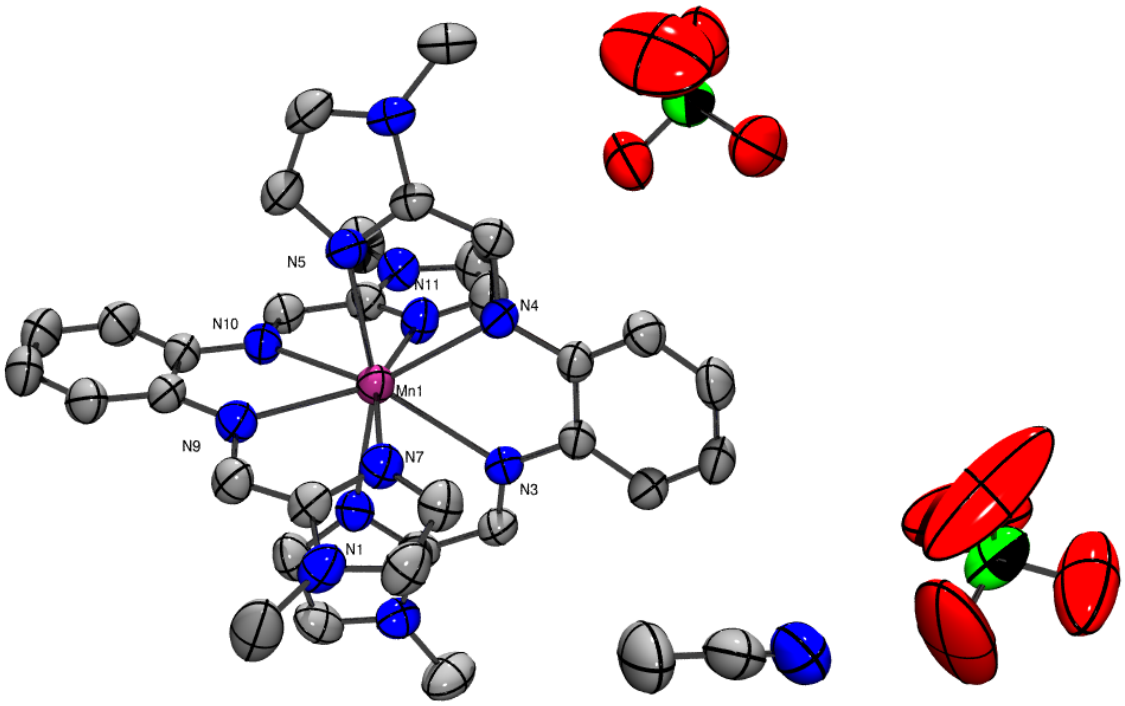

Fig. S5. ORTEP diagram of $[Mn(L_{N4})_2](ClO_4)_2$•MeCN (**1**•MeCN) at 50% thermal probability. H atoms have been omitted for clarity. Sphere color code: grey: C; red: O; blue: N; green: Cl; magenta: Mn.

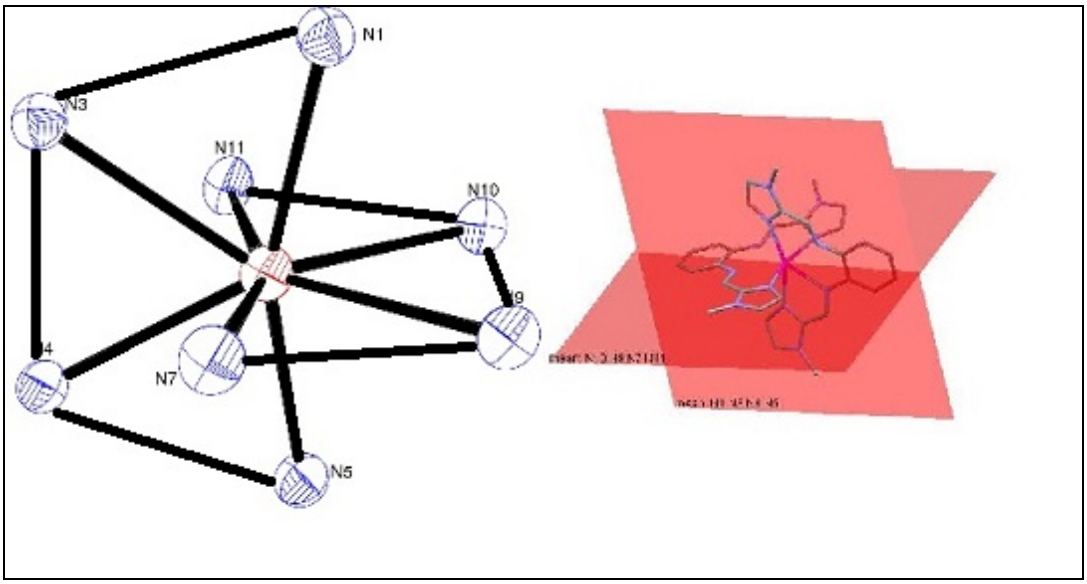

Fig. S6. (Left) A simplified view showing the coordination trapezoids (as defined by Lippard)[9] of the coordination sphere around Mn(II) in **1**; (Right) The two intersecting planes of the L_{N4} ligand in **1**; angle made by the two planes is 87.09°.

Relaxivity Measurements: The relaxivity measurements were carried out on a 60 MHz Varian EM360L-NMR spectrometer in a 5:1 CD_3OD/H_2O solvent mixture at 298 K using the standard saturation recovery pulse sequence (90°-τ-90°) where τ is the variable delay time. Each set of readings was taken 1 min after addition of complex **1** to the NMR tube. The data points were based on a predefined array of variable time delay intervals. The data was fit to 'T1 Inversion Recovery fitting three parameters' (T13IR).[10] The equation for the fit is:

$$y = A*\{1 - [1 + W*(1 - \exp(-K/T))]*\exp(-x/T)\} \qquad (\textbf{Eq.1})$$

where

T = T_1 relaxation time
A = H_2O peak integral at time x >> T
K = total time between scans in the 180-tau-90 sequence (equal to the acquisition time plus the relaxation delay time)
x = relaxation delay time t in the 180-tau-90 pulse sequence
W = -(integral at time x = 0/A); (W = percent inversion)

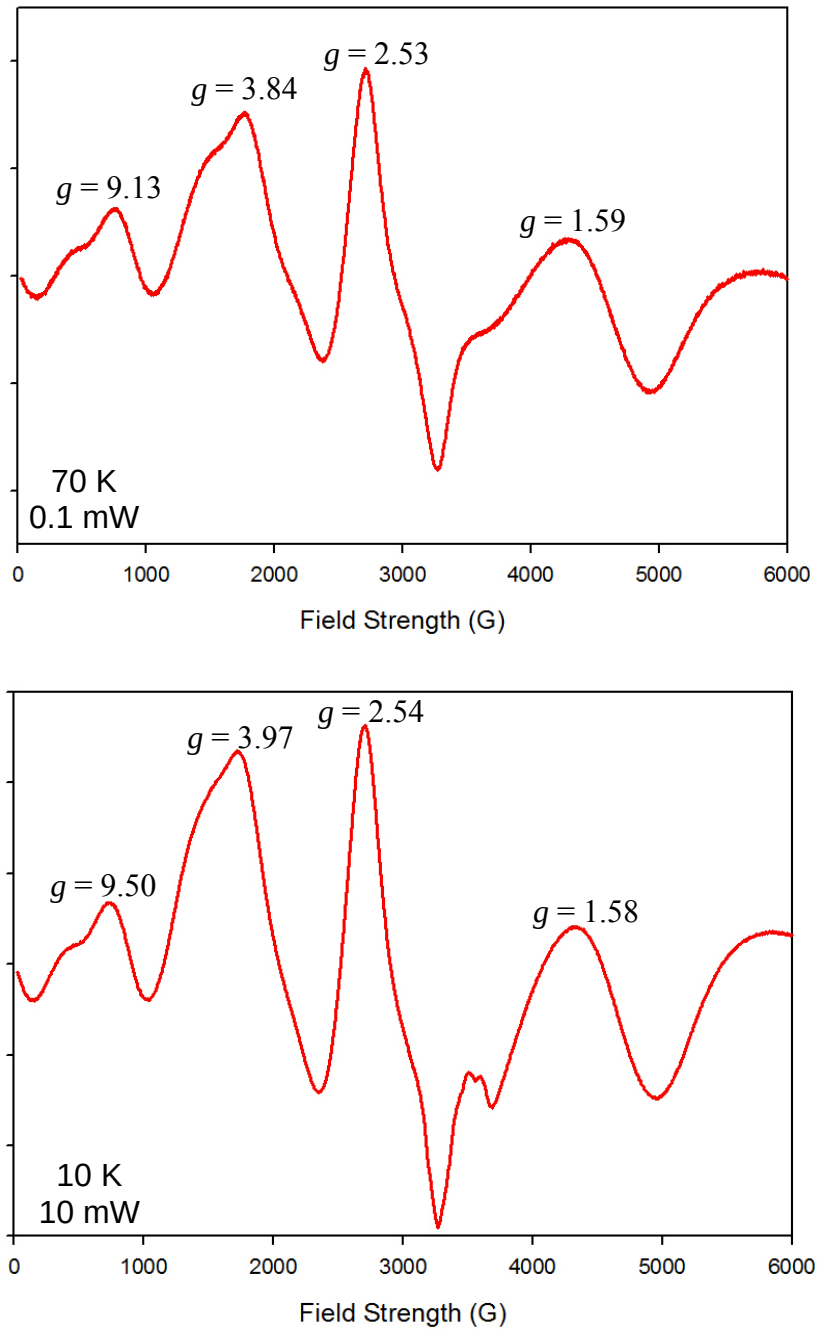

Fig. S7. X-band EPR spectrum of $[Mn(L_{N4})_2](ClO_4)_2$ (**1**) in a 1:1 MeCN:toluene glass at 70 K and 0.1 mW microwave power (top) and 10 K and 10 mW power (bottom). Microwave frequency = 9.6 GHz; modulation amplitude = 6.48 G. Selected *g*-values are displayed.

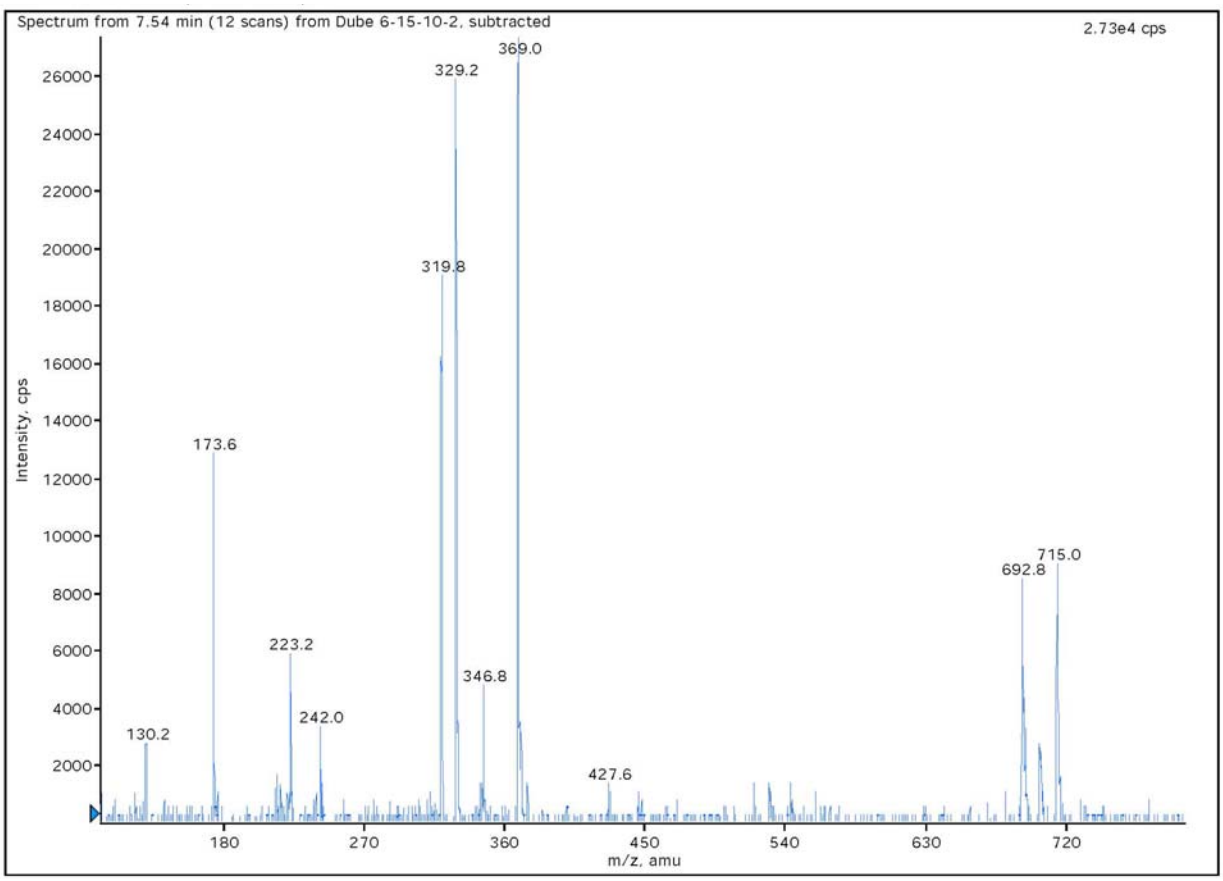

Fig. S8. Low-resolution ESI-MS of a 0.133 mM solution of $[Mn(L_{N4})_2](ClO_4)_2$ (**1**) in positive ion mode in pH 7.28 PIPES buffer after 2 h (solution from UV-vis studies). The *m/z* peak at 319.8 is consistent with $[Mn(L_{N4})_2]^{2+}$ (dication of **1**; calc *m/z* = 319.6); *m/z* peaks at 346.8 and 329.2 are consistent with aquated versions of **1**, namely $\{[Mn(L_{N4})_2]\bullet 3H_2O\}^{2+}$ (dication of **1•3H$_2$O**; calc. *m/z* = 346.6) and $\{[Mn(L_{N4})_2]\bullet H_2O\}^{2+}$ (dication of **1•H$_2$O**; calc. *m/z* = 328.6). The peak with *m/z* of 173.6 is consistent with the dication of $[Mn(L_{N4})]^{2+}$ (calc *m/z* = 173.6) via fragmentation of the parent ion **1**. There is no evidence for dissociated ligand (*m/z* = 293.2 for L_{N4} + H) or other ligand fragments in this spectrum. Other peaks have not been assigned, but can be attributed to the complexity of the reaction medium, which is buffered water.

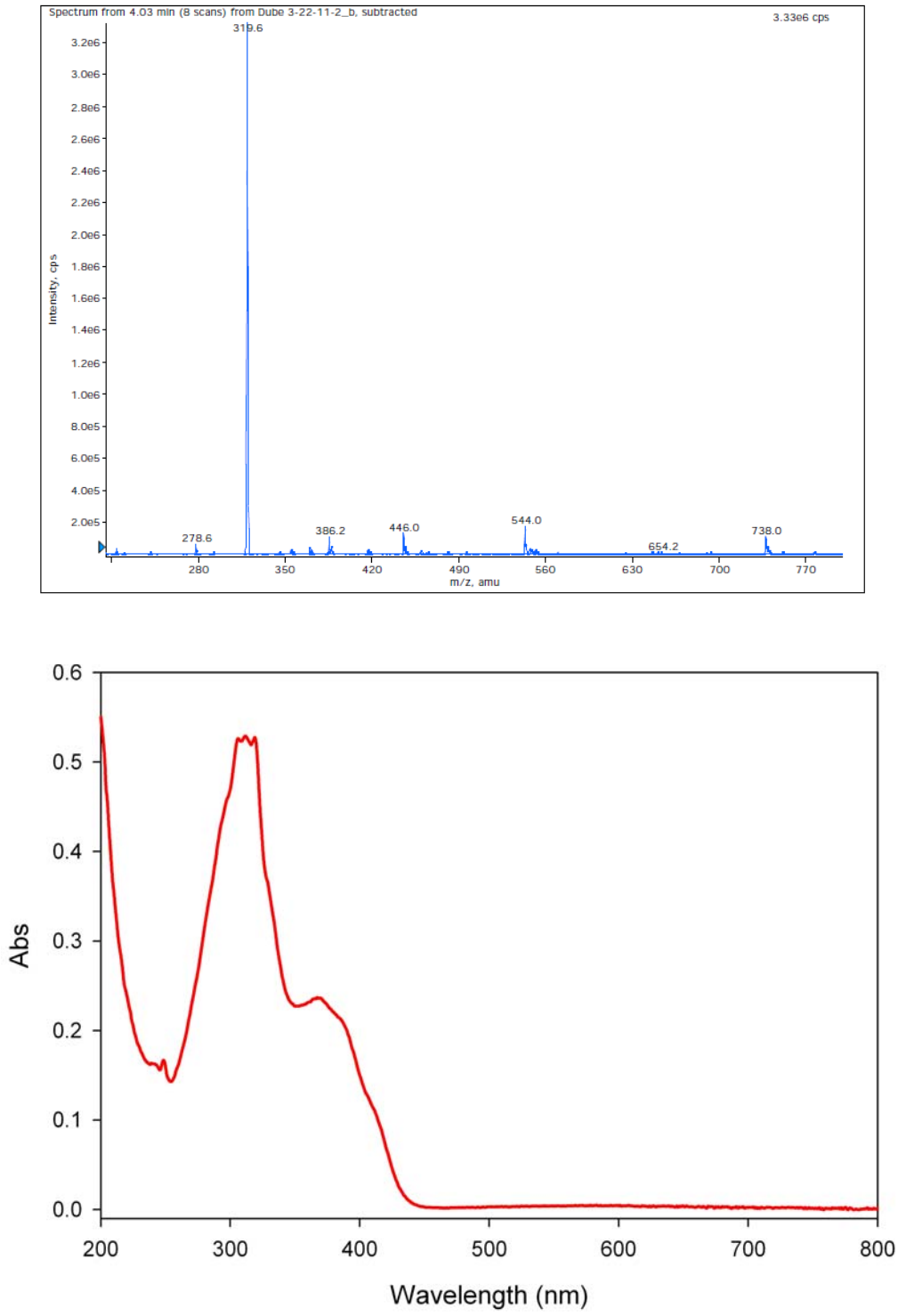

Fig. S9. (Top) Low-resolution ESI-MS(+) of the CH_2Cl_2 extract (see experimental for workup details) from a 0.133 mM solution of $[Mn(L_{N4})_2](ClO_4)_2$ (**1**) in pH 7.28 PIPES buffer after 2 h. The *m/z* peak at 319.6 is consistent with $[Mn(L_{N4})_2]^{2+}$ (dication of **1**; calc *m/z* = 319.6). (Bottom) qualitative UV-vis spectrum of the CH_2Cl_2 extract in MeCN at 298 K, which resembles the UV-vis of **1**.

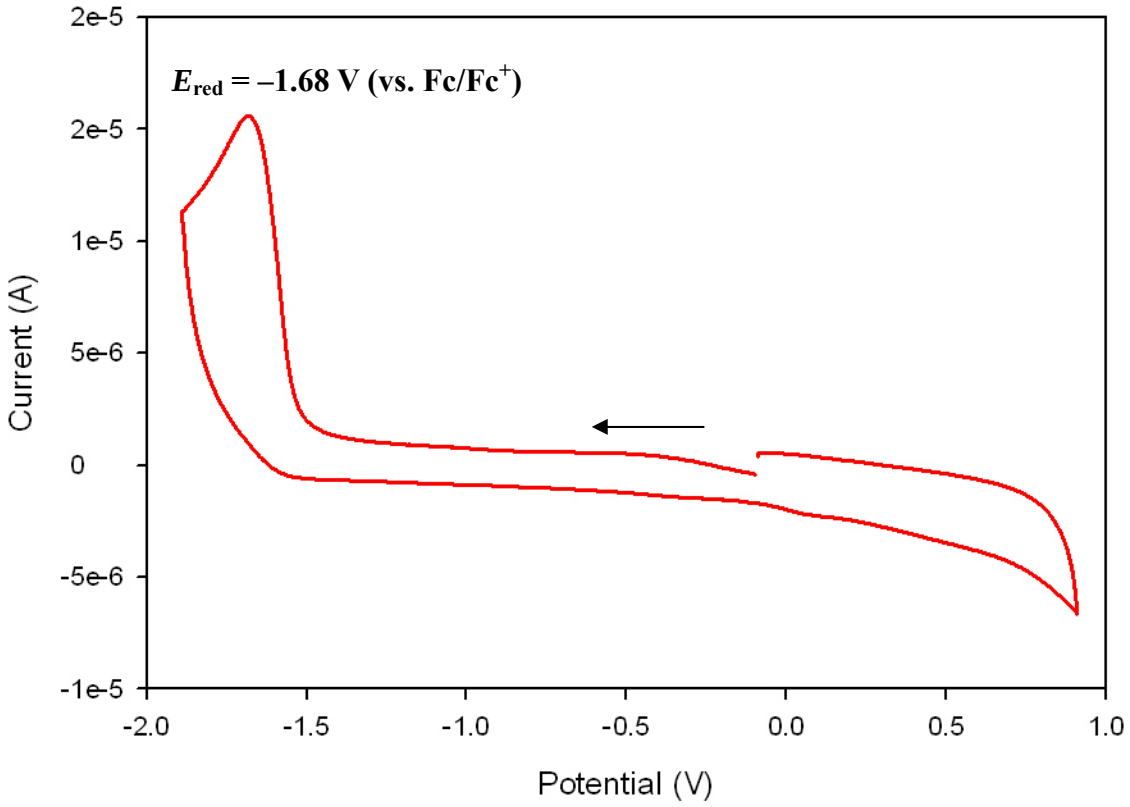

Fig. S10. Cyclic voltammogram of a 2.70 mM MeCN solution of $[Mn(L_{N4})_2](ClO_4)_2$ (**1**) (0.1 M $^nBu_4NPF_6$ supporting electrolyte, glassy carbon working electrode, Pt-wire counter electrode, RT, potential reported versus the ferrocene/ferrocenium couple). Arrow displays direction of scan.

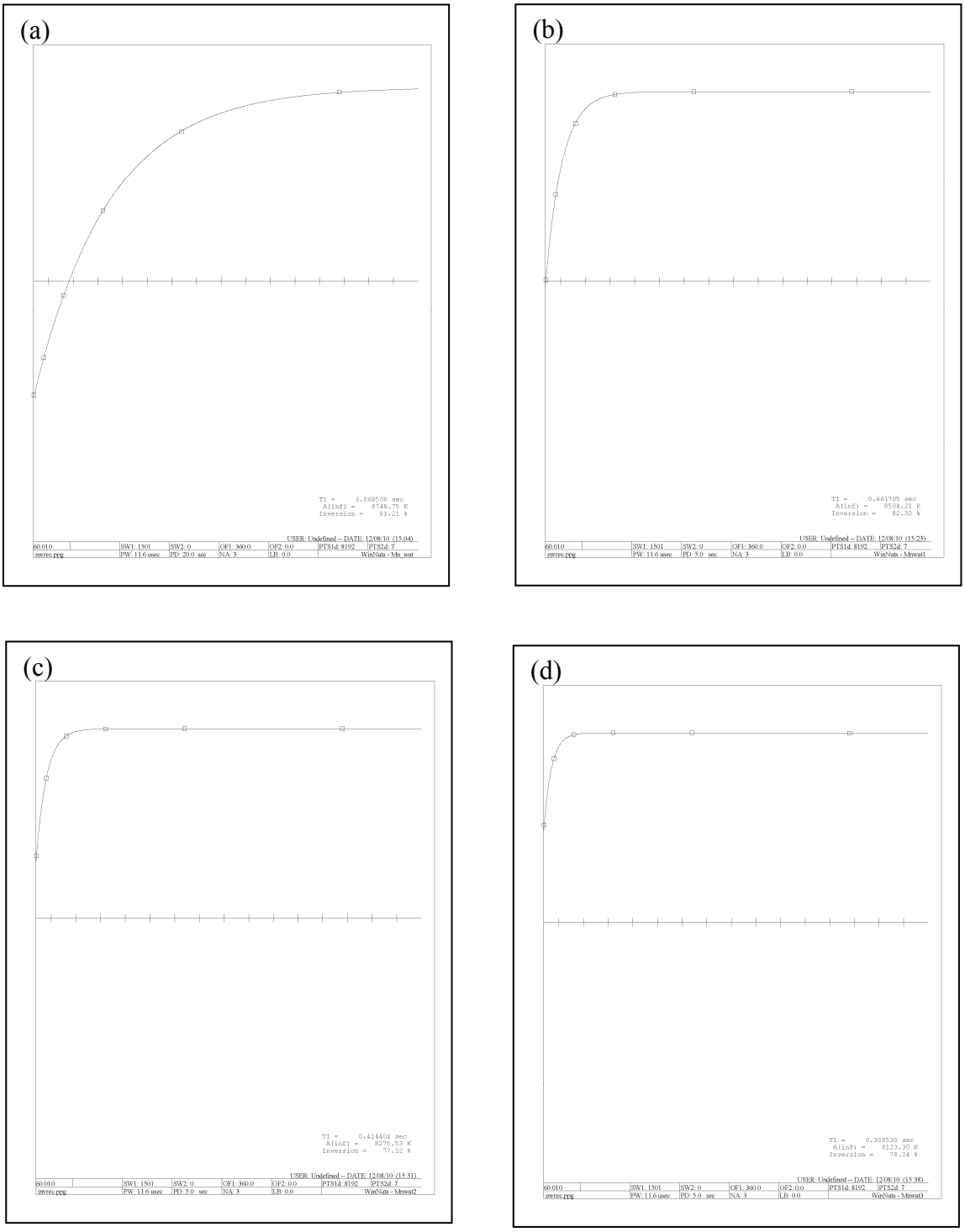

Fig. S11a-f. Representative plots for calculation of T1 relaxivity measurements for one sample run. The plots are ^{1}H signal integral of water versus time (s) fit according to Eq 1.

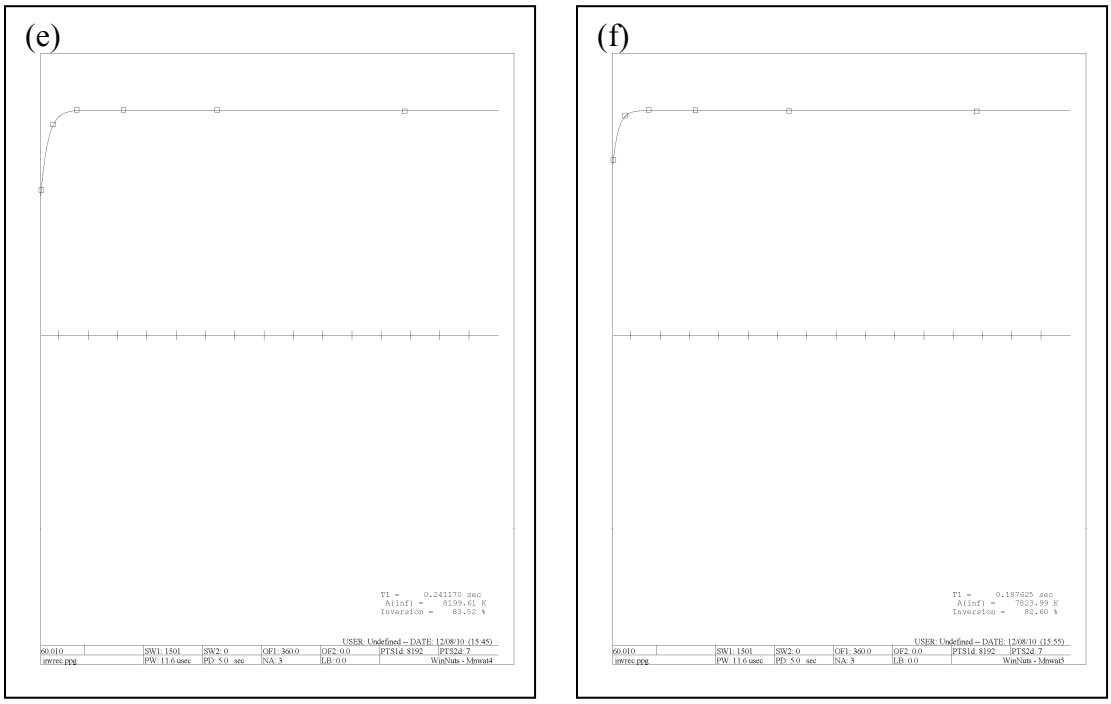

Fig. S11a-f (continued). Representative plots for calculation of T_1 relaxivity measurements for one sample run. The plots are ^{1}H signal integral of water versus time (s) fit according to Eq 1.

		R = 3.9419	
Plot	**Conc. (mM)**	**$1/T_1$ (s^{-1})**	**T_1**
(a)	0.0000	0.3259	3.0685
(b)	0.2607	1.5113	0.6617
(c)	0.5129	2.4131	0.4144
(d)	0.7572	3.2415	0.3085
(e)	0.9938	4.1465	0.2412
(f)	1.2231	5.3305	0.1876

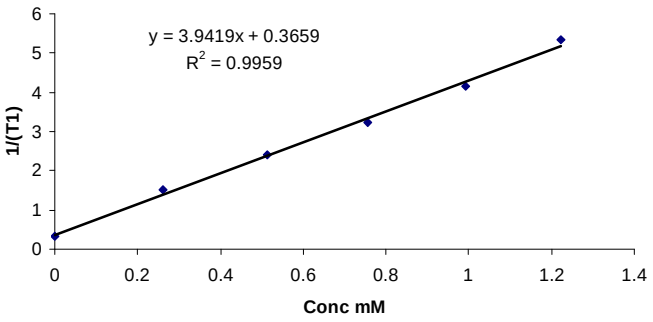

Fig. S12. Data and workup of one representative experiment to obtain the relaxivity (R_1) value for complex **1** (CD_3OD/H_2O (5:1), 60 MHz, 298 K).

References

(1) Patra, A. K.; Dube, K. S.; Papaefthymiou, G. C.; Conradie, J.; Ghosh, A.; Harrop, T. C. *Inorg. Chem.* **2010**, *49*, 2032.

(2) (a) Evans, D. F. *J. Chem. Soc.* **1959**, 2003. (b) Sur, S. K. *J. Magn. Resn.* **1989**, *82*, 169.

(3) *SMART v5.626: Software for the CCD Detector System*; Bruker AXS: Madison, WI, 2000.

(4) Walker, N.; Stuart, D. *Acta Crystallogr.* **1983**, *A39*, 158.

(5) Sheldrick, G. M. SADABS, Area Detector Absorption Correction, University of Göttingen, Göttingen, Germany, **2001**.

(6) Sheldrick, G. M. SHELX-97, Program for Refinement of Crystal Structures, University of Göttingen, Göttingen, Germany, **1997**.

(7) Sheldrick, G. M. SHELXTL 6.1, Crystallographic Computing System, Siemens Analytical X-Ray Instruments, Madison, WI, **2000**.

(8) Johnson, C. K. ORTEP-III, Report ORNL - 5138; Oak Ridge National Laboratory: Oak Ridge, TN, **1976**.

(9) Lippard, S. J. *Prog. Inorg. Chem.* **1967**, *8*, 109.

(10) (a) Levy, G. C.; Peat, I. R. *J. Magn. Reson.* **1975**, 18, 500. (b) http://www.acornnmr.com/NutsHelp/Relax.html